Journal of Microbiology (2022) Vol. 60, No. 1, pp. 128–136
DOI 10.1007/s12275-022-1620-3
eISSN 1976-3794
pISSN 1225-8873

Gold nanoparticle-DNA aptamer-assisted delivery of antimicrobial peptide effectively inhibits *Acinetobacter baumannii* infection in mice

Jaeyeong Park[1†], Eunkyoung Shin[1†], Ji-Hyun Yeom[1†], Younkyung Choi[1], Minju Joo[1], Minho Lee[2], Je Hyeong Kim[3], Jeehyeon Bae[4*], and Kangseok Lee[1*]

[1]*Department of Life Science, Chung-Ang University, Seoul 06974, Republic of Korea*
[2]*Department of Microbiology, College of Medicine, Hallym University, Chuncheon 24252, Republic of Korea*
[3]*Division of Pulmonology, Department of Internal Medicine, Korea University Ansan Hospital, Ansan 15355, Republic of Korea*
[4]*School of Pharmacy, Chung-Ang University, Seoul 06974, Republic of Korea*

(Received Nov 30, 2021 / Revised Dec 9, 2021 / Accepted Dec 13, 2021)

***Acinetobacter baumannii* causes multidrug resistance, leading to fatal infections in humans. In this study, we showed that Lys AB2 P3-His–a hexahistidine-tagged form of an antimicrobial peptide (AMP) loaded onto DNA aptamer-functionalized gold nanoparticles (AuNP-Apt)–can effectively inhibit *A. baumannii* infection in mice. When *A. baumannii*-infected mice were intraperitoneally injected with AuNP-Apt loaded with Lys AB2 P3-His, a marked reduction in *A. baumannii* colonization was observed in the mouse organs, leading to prominently increased survival time and rate of the mice compared to those of the control mice treated with AuNP-Apt or Lys AB2 P3-His only. This study shows that AMPs loaded onto AuNP-Apt could be an effective therapeutic tool against infections caused by multidrug-resistant pathogenic bacteria in humans.**

Keywords: *Acinetobacter baumannii*, antimicrobial peptide, gold nanoparticle, multidrug-resistant bacteria

Introduction

The World Health Organization (WHO) declared the antibiotic resistance of pathogenic bacteria as one of the most threatening human health issues (Bassetti *et al.*, 2011). The most common multidrug-resistant (MDR) bacteria are summarized under 'ESKAPE' : *Enterococcus faecium*, *Staphylococcus aureus*, *Klebsiella pneumoniae*, *Acinetobacter baumannii*, *Pseudomonas aeruginosa*, and *Enterobacter* spp. (Rice, 2008). Although the number of bacteria currently resistant to existing antibiotics has increased, only a few novel antibiotics have been discovered in the past 40 years due to the high cost and complexity associated with drug discovery and development (Projan, 2003; Lee *et al.*, 2019; Choi *et al.*, 2020). Unless the drug discovery pipeline produces new antibiotics to combat the growing problem of MDR bacteria, it will be challenging to treat infections caused by these pathogens (Fair and Tor, 2014; Shin and Park, 2017; Kim *et al.*, 2020; Lee *et al.*, 2021). Therefore, there is a need for novel therapeutic strategies, which can be obtained by developing new classes of antimicrobial compounds and efficient intracellular drug delivery systems.

Acinetobacter baumannii is a Gram-negative facultative anaerobe and opportunistic pathogen that is commonly found in the hospital environment and has recently been reported to present worldwide (Peleg *et al.*, 2008). Because of its ability to grow at different temperatures and pH conditions with minimal nutrients, *A. baumannii* can survive in dry conditions and in inanimate objects for up to 5 months (Jawad *et al.*, 1998; De Vegas *et al.*, 2006; Kramer *et al.*, 2006). Although adhesion is known to be the initial and critical step in *A. baumannii* infection, recent studies have shown that *A. baumannii* can invade host cells, such as the human lungs, larynx, and cervical epithelial cells (Choi *et al.*, 2008; Gaddy *et al.*, 2009), and become internalized into macrophages (Qiu *et al.*, 2012). This indicates that this bacterium also has an intracellular life cycle (Parra-Millán *et al.*, 2018). Infection of *A. baumannii* and its entry into the body through this route can eventually lead to serious hospital-acquired infections, such as ventilator-associated pneumonia, skin and soft tissue infections, bacteremia, surgical site infections, sepsis, urinary tract infections, and meningitis in humans (Valero *et al.*, 2001; Peleg *et al.*, 2008; Cerqueira and Peleg, 2011). It has been suggested that the mortality rate associated with *A. baumannii* infection is 20–70% (Fagon *et al.*, 1996; Blot *et al.*, 2003; Theaker *et al.*, 2003; Wang *et al.*, 2003; McConnell *et al.*, 2011).

In the past, *A. baumannii* was an easy-to-treat pathogen; however, it is now recognized as an MDR pathogen, with many strains being resistant to virtually all types of antibiotics available today, attracting worldwide attention as the cause of numerous outbreaks (Bergogne-Bérézin and Towner, 1996; Dijkshoorn *et al.*, 2007; Perez *et al.*, 2007). A final therapeutic option against MDR strains is the use of polymyxins, specifically colistin (polymyxin E) (Dijkshoorn *et al.*, 2007; Park *et al.*, 2010). Polymyxins, prescribed mostly in the 1960s and 1970s, were largely abandoned due to perceptions of toxicity, but have recently been reintroduced into human therapy with new and modified dosing regimens (Garnacho-Montero *et al.*, 2003; Esposito *et al.*, 2011). However, currently isolated

[†]These authors contributed equally to this work.
[*]For correspondence. (K. Lee) E-mail: kangseok@cau.ac.kr; Tel.: +82-2-820-5241; Fax: +82-2-825-5206 / (J. Bae) E-mail: jeehyeon@cau.ac.kr; Tel.: +82-2-820-5604; Fax: +82-2-816-7338

A. baumannii strains exhibit resistance to multiple drugs, including colistin (Mahgoub *et al.*, 2002; Park *et al.*, 2010; Rolain *et al.*, 2013). Thus, a new class of antibacterial agents has to be developed to prevent the spread of MDR strains of *A. baumannii* (MDRAB) (Wróblewska, 2006; Ko, 2019; Kim *et al.*, 2021).

Antimicrobial peptides (AMPs) are promising alternatives to conventional antibiotics (Hancock and Sahl, 2006; Kim *et al.*, 2019; Lemon *et al.*, 2019; Ryu *et al.*, 2021). AMPs are generally positively charged and amphipathic with short lengths (6–100 amino acids [aa]) (Gentilucci *et al.*, 2006; Kang *et al.*, 2017; Carratalá *et al.*, 2020). LysAB2 P3 is an AMP derived from the endolysin LysAB2 of *A. baumannii* phage, ΦAB2, which has antibacterial activity (Lai *et al.*, 2011). Among all the AMPs derived from LysAB2, LysAB2 P3 has the highest antibacterial activity against *A. baumannii*, with little hemolytic activity and no cytotoxic activity against mammalian cells (Peng *et al.*, 2017).

However, owing to the lack of a delivery system that prevents AMPs from rapid degradation in living systems, application of AMPs, including LysAB2 P3, in a clinical setting has been difficult (Roscia *et al.*, 2013; Mukhopadhyay *et al.*, 2020). Various nanomaterial-based systems have been developed to increase the delivery efficiency and stability of AMPs (Makabenta *et al.*, 2021). They are based on nanomaterials, such as dendrimers (Paleos *et al.*, 2004), polymers (Connor *et al.*, 2005), liposomes (Cheng *et al.*, 2006), nanorods (Schmid, 1992) and nanotubes (Rosi and Mirkin, 2005). However, in general, these systems require a complex process for loading AMPs onto nanocarriers and show low efficiency in inhibiting bacterial growth in *in vivo* models (Mishra *et al.*, 2017; Nordström and Malmsten, 2017).

To overcome the limitations of current nanomaterial-based systems for AMPs, our research group has developed a gold nanoparticle-DNA aptamer (AuNP-Apt) conjugate-based delivery system, which can easily load AMPs and increase the delivery efficiency and stability of AMPs (Yeom *et al.*, 2016; Lee *et al.*, 2017). In this study, we investigated whether this system could be used to relieve the *A. baumannii* infection in mice.

Materials and Methods

Synthesis of AuNP-Apt conjugates

Standard citrate-reduced AuNPs (15 nm in diameter) were purchased from BBI Solution (Crumlin). The anti-His (Kökpinar *et al.*, 2011) aptamer (5′-GCTATGGGTGGTCTGG TTGGGATTGGCCCCGGGAGCTGGC-A10-Thiol-3′) was purchased from Bioneer. The procedure for the synthesis of AuNP-Apt conjugates has been previously described (Yeom *et al.*, 2016).

Preparation of the AuNP-Apt-peptide complex

Solid-phase peptides were synthesized by GL Biochem. The procedure for the preparation of the AuNP-Apt-peptide complex has been previously described (Yeom *et al.*, 2016). Briefly, aptamer-conjugated AuNPs were pre-incubated at 80°C for 5 min to prevent the formation of secondary structures. AuNP-Apt^{His} (5 nM) and purified hexahistidine-tagged Lys AB2 P3 (16 μM) were incubated at room temperature in AMP-binding buffer (25 mM Tris-hydrogen chloride [HCl], pH 8.8, and 25 mM sodium hydroxide [NaOH]), which was equilibrated in 1 × phosphate-buffered saline (PBS) (137 mM sodium chloride [NaCl], 2.7 mM potassium chloride [KCl], 2 mM potassium dihydrogen phosphate [KH_2PO_4], pH 7.4, 10 mM disodium hydrogen phosphate [Na_2HPO_4]) for 10 min. The pH of each solution was adjusted using HCl.

Binding capacity assay

The procedure for the binding capacity assay has been previously described (Yeom *et al.*, 2016). Briefly, AuNP-Apt^{His} (5 nM) was hybridized with increasing concentrations of AMP (0, 1, 2, 4, 8, and 16 μM), and the resulting conjugates were resolved by tricine-sodium dodecyl sulfate-polyacrylamide gel electrophoresis (Tricine-SDS-PAGE) and analyzed by western blotting. The membranes were immunoblotted with anti-His antibody (Santa Cruz Biotechnology; Qiagen). The signal was developed with an electrochemiluminescent reagent. Band intensity was measured using Quantity One software (Bio-Rad).

Antibacterial assay

Acinetobacter baumannii C078 cells were cultured at 37°C in tryptic soy broth (TSB) medium, and the minimum inhibitory concentration (MIC) of each peptide was determined using microdilution assays (Jiang *et al.*, 2019). Briefly, two-fold serial dilutions covering a range from 1–16 μM for each peptide were added to duplicate bacteria-containing media (1×10^3 colony forming units [CFU]/ml) in the mid-logarithmic phase of growth. The samples were then incubated for 18–24 h at 37°C. After incubation, MICs were determined as the lowest concentration of peptide based on OD_{600} measurements of the cultures.

Stability of peptide in serum

The aqueous peptide (50 μM) and AuNP-Apt-peptide (50 μM) complexes were incubated in Dulbecco's modified Eagle's medium (DMEM) (Welgene) containing 10% (v/v) fetal bovine serum (FBS) (Welgene) at 37°C. After 0, 3, 6, 9, and 12 h, each peptide and serum were separated Tricine-SDS-PAGE and analyzed by western blotting.

Mammalian cell culture

HeLa (human cervical carcinoma) cells were cultured in DMEM (Welgene) supplemented with 10% (v/v) FBS (Welgene) and 1% (v/v) penicillin-streptomycin (Welgene) at 37°C with 5% (v/v) carbon dioxide (CO_2) in humidified air.

Cytotoxicity assay

The procedure for the cytotoxicity assay has been previously described (Yeom *et al.*, 2016). Briefly, HeLa (1.2×10^4/well) cells were plated and cultured for 18–24 h in 96-well culture dishes. Subsequently, cells were incubated for an additional 24 h with peptides in the culture medium. Cell viability assay was performed using a CellTiter-Glo® luminescent cell viability assay kit (Promega).

In vitro infection assay: viable intracellular bacteria cell count assay

HeLa cells (1×10^5/well) were plated and cultured in 24-well plates for 18–24 h. HeLa cells were infected with *A. baumannii* for 30 min at a 1:10 multiplicity of infection (MOI). The cells were then washed twice with DMEM containing 50 mg/ml gentamicin (Gibco^{TM}, Invitrogen). Next, the cells were incubated in DMEM medium containing 10% (v/v) FBS with the AuNP-Apt-AMP complex or control reagents for 5 h. To remove any remaining antimicrobial peptides and extracellular bacteria, the cells were washed three times with 1 × PBS. Then, HeLa cells were lysed in a PBS solution containing 1% (v/v) Triton X-100 to release of intracellular bacteria from the cells. The bacterial cells were then diluted in PBS and plated onto TSB plates to determine the number of CFU.

In vitro infection assay: infected cell viability assay

HeLa cells (1×10^5/well) were seeded and grown in 24-well cell culture plates for 18–24 h. HeLa cells were then either treated with the buffer or infected with *A. baumannii* for 30 min at a 1:10 MOI. The cells were washed twice with 1 × PBS, once with DMEM medium containing 50 mg/ml gentamicin (Gibco^{TM}). Then, the cells were cultured in DMEM medium containing 10% (v/v) FBS with the AuNP-Apt-AMP complex or control reagents for 24 h. The cells were detached by trypsin-ethylenediaminetetraacetic acid (EDTA), and viability was measured by Trypan Blue (TB) dye exclusion assay.

Animals

Seven-week-old female ICR mice (DBL), weighing 18–20 g,

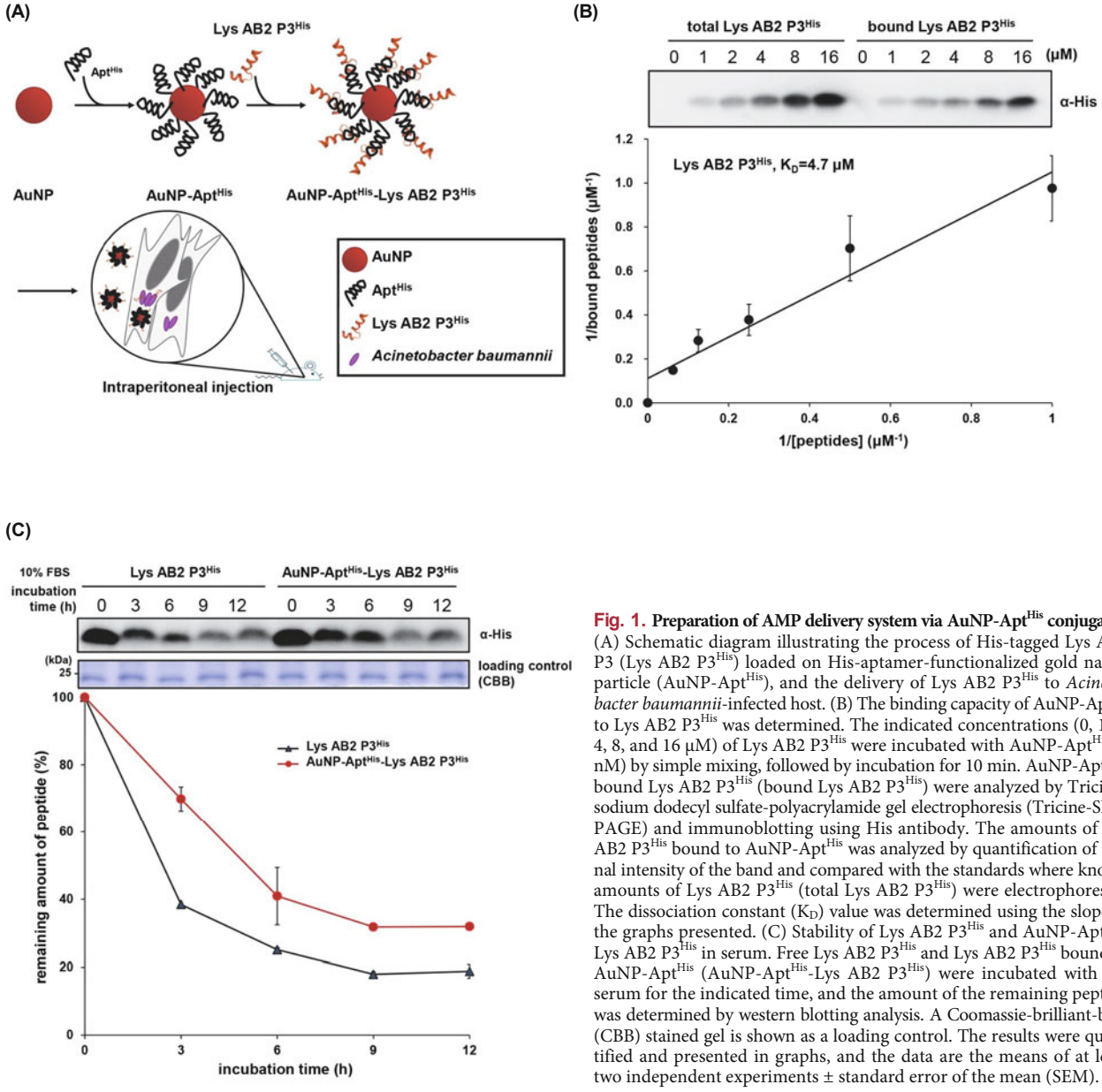

Fig. 1. Preparation of AMP delivery system via AuNP-Apt^{His} conjugates. (A) Schematic diagram illustrating the process of His-tagged Lys AB2 P3 (Lys AB2 P3^{His}) loaded on His-aptamer-functionalized gold nanoparticle (AuNP-Apt^{His}), and the delivery of Lys AB2 P3^{His} to *Acinetobacter baumannii*-infected host. (B) The binding capacity of AuNP-Apt^{His} to Lys AB2 P3^{His} was determined. The indicated concentrations (0, 1, 2, 4, 8, and 16 μM) of Lys AB2 P3^{His} were incubated with AuNP-Apt^{His} (5 nM) by simple mixing, followed by incubation for 10 min. AuNP-Apt^{His}-bound Lys AB2 P3^{His} (bound Lys AB2 P3^{His}) were analyzed by Tricine-sodium dodecyl sulfate-polyacrylamide gel electrophoresis (Tricine-SDS-PAGE) and immunoblotting using His antibody. The amounts of Lys AB2 P3^{His} bound to AuNP-Apt^{His} was analyzed by quantification of signal intensity of the band and compared with the standards where known amounts of Lys AB2 P3^{His} (total Lys AB2 P3^{His}) were electrophoresed. The dissociation constant (K_D) value was determined using the slope of the graphs presented. (C) Stability of Lys AB2 P3^{His} and AuNP-Apt^{His}-Lys AB2 P3^{His} in serum. Free Lys AB2 P3^{His} and Lys AB2 P3^{His} bound to AuNP-Apt^{His} (AuNP-Apt^{His}-Lys AB2 P3^{His}) were incubated with the serum for the indicated time, and the amount of the remaining peptide was determined by western blotting analysis. A Coomassie-brilliant-blue (CBB) stained gel is shown as a loading control. The results were quantified and presented in graphs, and the data are the means of at least two independent experiments ± standard error of the mean (SEM).

Table 1. Antibacterial activities of synthetic peptides and antibiotics.

Peptides	Sequences	$M.W_a$	MIC_b (μM)
Lys AB2 P3	NPEKALEKLIAIQKAIKGMLNGWFTGVGFRRKR	3771.57	2–4
Lys AB2 $P3^{His}$	NPEKALEKLIAIQKAIKGMLNGWFTGVGFRRKRHHHHHH	4594.42	2–4
Antibiotics	Classification	$M.W_a$	MIC_b (μM)
Ampicillin	Penicillins	349.4	> 256
Erythromycin	Macrolides	733.9	> 256

$M.W_a$, molecular weight.
MIC_b, minimal inhibitory concentration.

were used for *in vivo* studies. Mice were housed in a room, which was maintained at a humidity of 30–40% (v/v) and a temperature of 22 ± 1°C. The lighting in the room was on a 12-h light/12-h dark cycle (12L:12D). All experimental procedures were reviewed and approved by the Chung-Ang University Support Center for Animal Experiments, and all research methods have been conducted in accordance with the guidelines and regulations. Animal handling guidelines were approved by the Chung-Ang University Institutional Animal Case and Use Committee (Approval #CAU2020-00115).

In vivo infection assay

Thirty min after the bacterial challenge, AuNP-Apt-AMP complexes (3 mg/kg) and control reagents were intraperitoneally injected twice in 2 h. The mice were carefully monitored after infection and euthanized immediately if they became moribund.

In vivo infection assay: viable bacterial cell count assay

Inoculation of *A. baumannii* C078 was grown in TSB until the mid-log phase and washed with PBS. All mice were deprived of food and water for 4–18 h before bacterial infection. The mice were then infected with 100 ml of PBS containing 1×10^8 CFU of *A. baumannii* intraperitoneally (i.p.). Thirty min after the bacterial challenge, AuNP-Apt-AMP complexes (3 mg/kg) and control reagents were injected i.p. once a day. Five h after the bacterial challenge, control, Lys AB2 $P3^{His}$, or AuNP-Apt^{His}-Lys AB2 $P3^{His}$-treated mice were killed, and the spleen and lungs were removed. The organs were weighed, gently washed in PBS, and then homogenized separately. Homogenates were plated on TSB agar. Plates were incubated at 37°C overnight, and colonies counted. Results are expressed as the number of CFU/g. This assay was repeated three times.

Statistical analysis

Data were presented as mean ± standard error of the mean (SEM). Student's *t*-test (Excel; Microsoft Corp.) was used, and $P < 0.05$ was considered statistically significant.

Results

Antibacterial activity of Lys AB2 $P3^{His}$ against *A. baumannii*

The C-terminal end of Lys AB2 P3 was tagged with hexahistidine (His) to load Lys AB2 P3 onto the AuNP-Apt^{His} conjugate via interaction of a His-tagged Lys AB2 P3 (Lys AB2 $P3^{His}$) with a His aptamer (Apt^{His}) (Fig. 1A). The bactericidal activity of Lys AB2 $P3^{His}$ against *A. baumannii* was tested by measuring the MICs. The MICs of Lys AB2 $P3^{His}$ for *A. baumannii* strains were in the range of 2–4 μM, which were much lower than those of ampicillin and erythromycin, indicating higher antibacterial activity of Lys AB2 $P3^{His}$ (Table 1). His tagging of Lys AB2 P3 did not alter the MIC of *A. baumannii.*

In vitro antibacterial action of the AuNP-Apt-Lys AB2 $P3^{His}$ complex on *A. baumannii*-infected mammalian cells

To apply the tagged-AMP delivery system using AuNP-Apt^{His}, we first checked the binding affinity of Lys AB2 $P3^{His}$ to AuNP-Apt^{His}. The results showed that approximately 50–55% of the Lys AB2 $P3^{His}$ in the reaction mixture were bound to AuNP-Apt^{His} (Fig. 1B). Under these reaction conditions, the dissociation constant (K_D) for the AuNP-Apt^{His}-Lys AB2 $P3^{His}$ complex was estimated to be 4.7 μM. We further tested whether the stability of Lys AB2 $P3^{His}$ could be improved when loaded onto AuNP-Apt^{His} by measuring the amount of intact Lys AB2 $P3^{His}$ in the serum during 12 h of incubation. Detection of Lys AB2 $P3^{His}$ by western blotting showed a sharp decrease in intact Lys AB2 $P3^{His}$ when not loaded onto AuNP-Apt^{His}, and as a result, ~60% of the peptide degraded after 3 h incubation in the serum ($t_{1/2}$ = 2.44 h) (Fig. 1C). The degradation of Lys AB2 $P3^{His}$ loaded onto AuNP-Apt^{His} conjugates in the serum was slower than that of Lys AB2 $P3^{His}$ itself: ~70% of Lys AB2 $P3^{His}$ remained in serum after 3 h of incubation. These results suggest that AuNP-Apt^{His} contributes to improving the stability of Lys AB2 $P3^{His}$.

To examine the effects of AuNP-Apt^{His}-Lys AB2 $P3^{His}$ on *A. baumannii*-infected cells, we first evaluated the cytotoxicity of AuNP-Apt^{His}-Lys AB2 $P3^{His}$ in HeLa cells. The results of the cell viability assay in mammalian cells showed that Lys AB2 $P3^{His}$ and AuNP-Apt^{His}-Lys AB2 $P3^{His}$ did not exhibit cytotoxicity against HeLa cells (Fig. 2A). Next, we treated *A. baumannii*-infected HeLa cells with the buffer, Lys AB2 P3, Lys AB2 $P3^{His}$, AuNP-Apt^{His}, or AuNP-Apt^{His}-Lys AB2 $P3^{His}$ for 5 h. Viable intracellular *A. baumannii* cells were counted by measuring the CFUs. The number of intracellular *A. baumannii* cells in the AuNP-Apt^{His}-Lys AB2 $P3^{His}$-treated cells was approximately 50% lower than that in the AuNP-Apt^{His}-treated cells (Fig. 2B). The treatment of *A. baumannii*-infected HeLa cells with Lys AB2 $P3^{His}$ alone resulted in an approximately 25% reduction in viable intracellular bacteria than that in the buffer-treated HeLa cells, indicating the ability of Lys AB2 $P3^{His}$ to inhibit the growth of intracellular *A. baumannii* cells, as has been previously reported for Lys AB2 P3 (Peng *et al.*, 2017). These results show that AuNP-Apt^{His} conjugates can efficiently deliver Lys AB2 $P3^{His}$ into HeLa cells and, consequently, enhance their bactericidal activity against

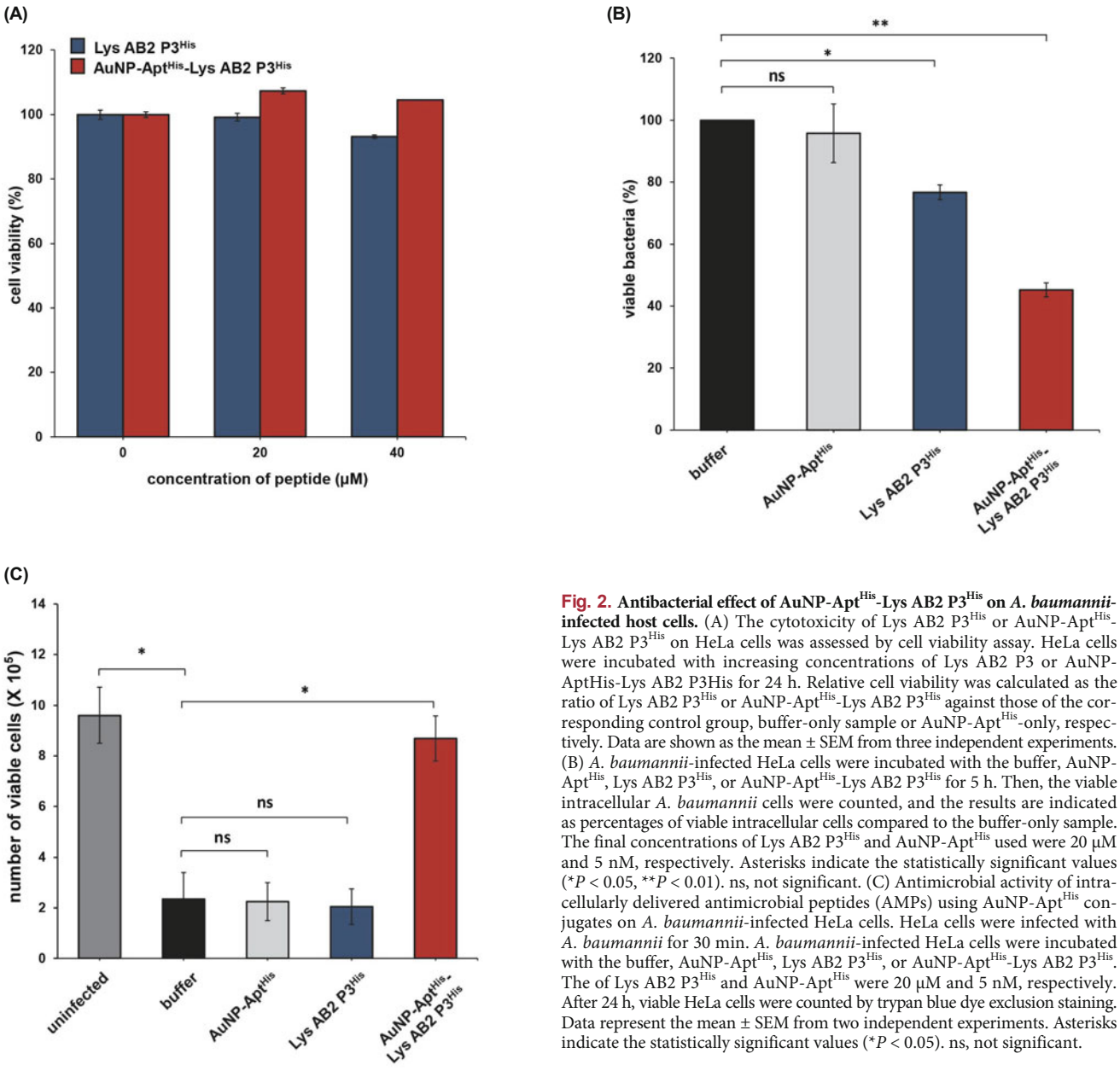

Fig. 2. Antibacterial effect of AuNP-Apt^{His}-Lys AB2 P3^{His} on *A. baumannii*-infected host cells. (A) The cytotoxicity of Lys AB2 P3^{His} or AuNP-Apt^{His}-Lys AB2 P3^{His} on HeLa cells was assessed by cell viability assay. HeLa cells were incubated with increasing concentrations of Lys AB2 P3 or AuNP-AptHis-Lys AB2 P3His for 24 h. Relative cell viability was calculated as the ratio of Lys AB2 P3^{His} or AuNP-Apt^{His}-Lys AB2 P3^{His} against those of the corresponding control group, buffer-only sample or AuNP-Apt^{His}-only, respectively. Data are shown as the mean ± SEM from three independent experiments. (B) *A. baumannii*-infected HeLa cells were incubated with the buffer, AuNP-Apt^{His}, Lys AB2 P3^{His}, or AuNP-Apt^{His}-Lys AB2 P3^{His} for 5 h. Then, the viable intracellular *A. baumannii* cells were counted, and the results are indicated as percentages of viable intracellular cells compared to the buffer-only sample. The final concentrations of Lys AB2 P3^{His} and AuNP-Apt^{His} used were 20 μM and 5 nM, respectively. Asterisks indicate the statistically significant values (*P < 0.05, **P < 0.01). ns, not significant. (C) Antimicrobial activity of intracellularly delivered antimicrobial peptides (AMPs) using AuNP-Apt^{His} conjugates on *A. baumannii*-infected HeLa cells. HeLa cells were infected with *A. baumannii* for 30 min. *A. baumannii*-infected HeLa cells were incubated with the buffer, AuNP-Apt^{His}, Lys AB2 P3^{His}, or AuNP-Apt^{His}-Lys AB2 P3^{His}. The of Lys AB2 P3^{His} and AuNP-Apt^{His} were 20 μM and 5 nM, respectively. After 24 h, viable HeLa cells were counted by trypan blue dye exclusion staining. Data represent the mean ± SEM from two independent experiments. Asterisks indicate the statistically significant values (*P < 0.05). ns, not significant.

intracellular *A. baumannii* cells.

We further examined whether the treatment of *A. baumannii*-infected HeLa cells with AuNP-Apt^{His}-Lys AB2 P3^{His} can lead to increased cell viability. *A. baumannii*-infected HeLa cells were treated with the buffer, AuNP-Apt^{His}, Lys AB2 P3^{His}, or AuNP-Apt^{His}-Lys AB2 P3^{His}, and viable HeLa cells were counted by trypan blue exclusion assay after 24 h (Fig. 2C). In the case of AuNP-Apt^{His}-Lys AB2 P3^{His}-treated cells, the number of surviving HeLa cells increased more than 3.6-fold compared to the cells treated with only buffer 24 h post-treatment. This result is compatible with that of HeLa cells uninfected with *A. baumannii*. When treated with AuNP-Apt^{His} or Lys AB2 P3^{His} only, the number of viable HeLa cells 24 h post-infection was reduced by approximately 80% compared to uninfected cells. Taken together, these results showed an increase in the intracellular antibacterial activity of Lys AB2 P3^{His} by AuNP-Apt^{His} conjugates and, consequently, in the viability of *A. baumannii*-infected HeLa cells.

In vivo bactericidal action of the AuNP-Apt-Lys AB2 P3^{His} complex in *A. baumannii*-infected mice

To investigate whether this system can be applied to animals as an antibacterial therapy, we utilized a mouse model of *A. baumannii* infection. First, mice were infected via the intraperitoneal injection of *A. baumannii* (1×10^8 CFU), and the spread of *A. baumannii* cells in the organs of mice, including the liver, lung, and spleen, was monitored for 4 h after inoculation. As shown in Fig. 3A, inoculated *A. baumannii* cells sufficiently colonized these organs as early as 30 min. Next, to verify the *in vivo* treatment effect of AuNP-Apt^{His}-Lys AB2

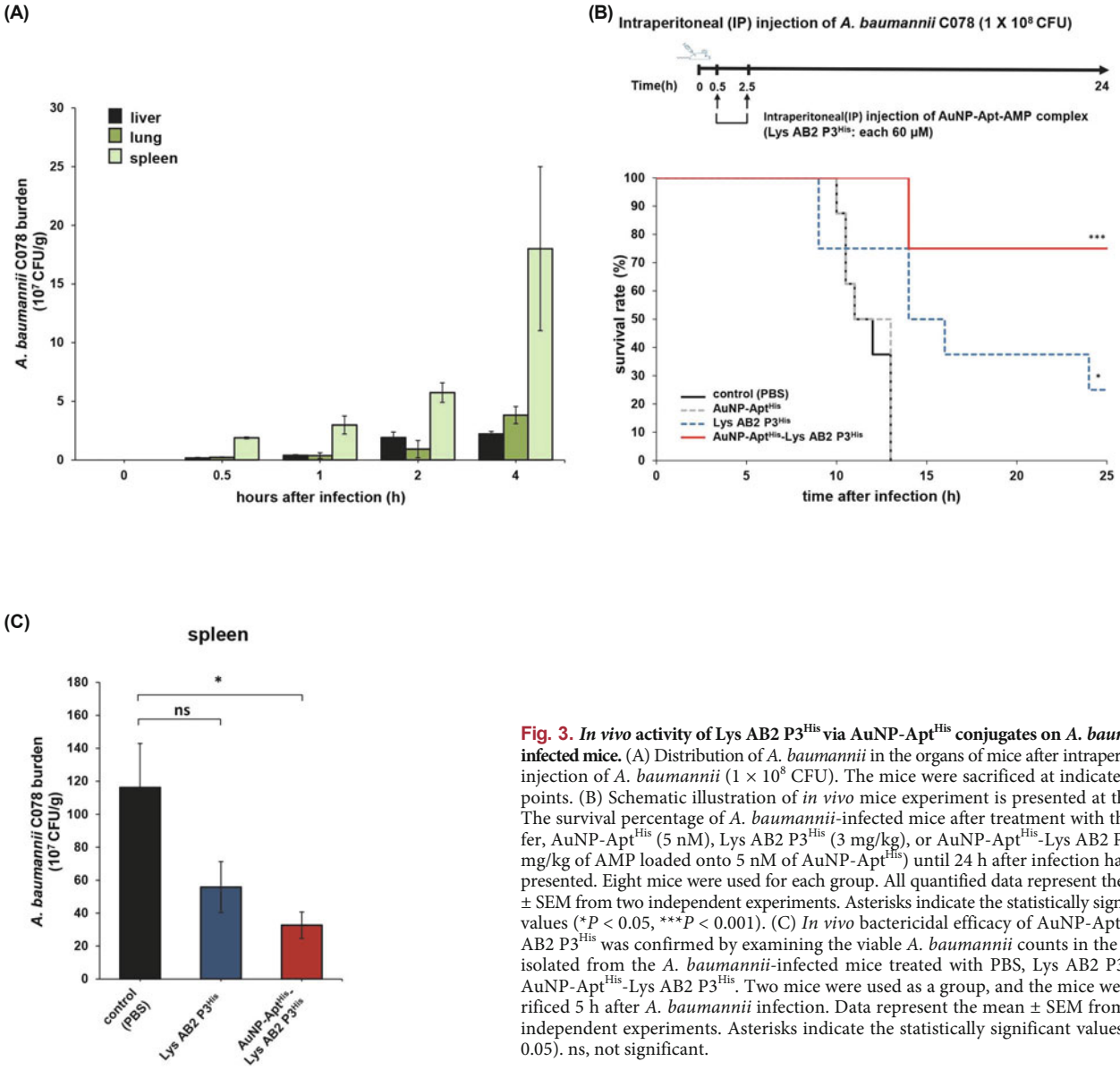

Fig. 3. ***In vivo*** **activity of Lys AB2 P3^{His} via AuNP-Apt^{His} conjugates on *A. baumannii* infected mice.** (A) Distribution of *A. baumannii* in the organs of mice after intraperitoneal injection of *A. baumannii* (1×10^8 CFU). The mice were sacrificed at indicated time points. (B) Schematic illustration of *in vivo* mice experiment is presented at the top. The survival percentage of *A. baumannii*-infected mice after treatment with the buffer, AuNP-Apt^{His} (5 nM), Lys AB2 P3^{His} (3 mg/kg), or AuNP-Apt^{His}-Lys AB2 P3^{His} (3 mg/kg of AMP loaded onto 5 nM of AuNP-Apt^{His}) until 24 h after infection has been presented. Eight mice were used for each group. All quantified data represent the mean ± SEM from two independent experiments. Asterisks indicate the statistically significant values (*$P < 0.05$, ***$P < 0.001$). (C) *In vivo* bactericidal efficacy of AuNP-Apt^{His}-Lys AB2 P3^{His} was confirmed by examining the viable *A. baumannii* counts in the spleen isolated from the *A. baumannii*-infected mice treated with PBS, Lys AB2 P3^{His}, or AuNP-Apt^{His}-Lys AB2 P3^{His}. Two mice were used as a group, and the mice were sacrificed 5 h after *A. baumannii* infection. Data represent the mean ± SEM from three independent experiments. Asterisks indicate the statistically significant values (*$P < 0.05$). ns, not significant.

P3^{His}, 30 min after inoculation of *A. baumannii* cells, the buffer, AuNP-Apt^{His}, Lys AB2 P3^{His}, or AuNP-Apt^{His}-Lys AB2 P3^{His} were injected twice with an interval of 2 h (Fig. 3B). Then, the survival rate of the mice was observed for 25 h. All infected mice injected with buffer or AuNP-Apt^{His} died before 13 h post-infection. In contrast, more than 70% of the infected mice survived for up to 25 h when treated with AuNP-Apt^{His}-Lys AB2 P3^{His}. In mice injected with Lys AB2 P3^{His} alone, the survival rate was slightly higher than that in mice injected with the buffer or AuNP-Apt^{His} alone, resulting in a 20% survival rate up to 25 h post-infection. To examine whether the increased survival rate of *A. baumannii*-infected mice when treated with AuNP-Apt^{His}-Lys AB2 P3^{His} stems from the inhibition of *A. baumannii* growth, the number of viable *A. baumannii* cells was measured in homogenates of these mice at 5 h post-infection (Fig. 3C). In mice treated with AuNP-Apt^{His}-Lys AB2 P3^{His}, the number of viable *A. baumannii* cells in the spleen was reduced by 3.5-fold compared to that in mice treated with the buffer. These results demonstrate that the intraperitoneal injection of Lys AB2 P3^{His}-loaded AuNP-Apt^{His} conjugates was effective in preventing the colonization of *A. baumannii* cells in mice, which consequently increased the survival of *A. baumannii*-infected mice.

Discussion

In recent years, *Acinetobacter* species, particularly *A. baumannii*, have become "red alert" human pathogens, owing to their ability to develop resistance to all currently available antibiotics (Cerqueira and Peleg, 2011). It is suspected that the existence of intracellular *A. baumannii* cells is a reason for the decrease in the therapeutic efficacy of antibiotics due

to the poor uptake of the compounds into infected host cells (Darouiche and Hamill, 1994; Choi *et al.*, 2008; Gaddy *et al.*, 2009; Xiong *et al.*, 2014; Lehar *et al.*, 2015). Therefore, there is a need for more effective antibacterial agents and their delivery systems for the treatment of infections with MDR strains of *A. baumannii*.

The broad-spectrum activity, hydrophobicity, and rapid killing kinetics of AMPs result in enhanced selectivity and activity against pathogens, making them attractive antimicrobial agents (Almaaytah *et al.*, 2017; Ryu *et al.*, 2021). However, there are limitations in the development and clinical use of AMPs, such as low antimicrobial target selectivity, high systemic toxicity, low stability, and the lack of an efficient *in vivo* delivery system for AMPs (Marr *et al.*, 2006; Yeung *et al.*, 2011; Kang *et al.*, 2014).

In this study, we used an AuNP-Apt conjugate-based delivery system (Yeom *et al.*, 2016; Lee *et al.*, 2017) to overcome the limitations of current delivery systems for AMPs. We showed that the growth of *A. baumannii* can be effectively and efficiently inhibited in mice through the combination of the *A. baumannii*-targeting peptide Lys AB2 $P3^{His}$ and the AuNP-Apt delivery system. Thus, using the AuNP-Apt delivery system, the *in vivo* delivery strategy–binding to a specific bacterium-targeting AMP–can be applied to various other MDR bacteria, such as *P. aeruginosa* and *S. aureus*. For better application of the AuNP-Apt delivery system, further studies are needed to discover DNA aptamers that can specifically bind to AMPs to minimize changes in the antibacterial activity by adding a tag (e.g., hexahistidine) to AMPs.

Acknowledgements

We thank Drs. Minkyung Ryu and Hanyong Jin for their technical assistance on this work. This research was supported by the Chung-Ang University Graduate Research Scholarship grants in 2020 and the National Research Foundation of Korea [NRF-2021R1A2C3008934 to K. L. and NRF-2021R1-I1A1A01056162 to J-H. Y].

Conflict of Interest

The authors declare that they have no conflicts of interest.

Ethical Statements

All experimental procedures were reviewed and approved by the Chung-Ang University Support Center for Animal Experiments, and all research methods have been conducted in accordance with the guidelines and regulations. Animal handling guidelines were approved by the Chung-Ang University Institutional Animal Case and Use Committee (Approval #CAU2020-00115).

References

Almaaytah, A., Mohammed, G.K., Abualhaijaa, A., and Al-Balas, Q. 2017. Development of novel ultrashort antimicrobial peptide nanoparticles with potent antimicrobial and antibiofilm activities against multidrug-resistant bacteria. *Drug Des. Devel. Ther.* **11**, 3159–3170.

Bassetti, M., Ginocchio, F., and Mikulska M. 2011 New treatment options against Gram-negative organisms. *In* Vincent, J.L. (ed.), Annual Update in Intensive Care and Emergency Medicine 2011, vol. 1. Springer, Berlin, Germany.

Bergogne-Bérézin, E. and Towner, K.J. 1996. *Acinetobacter* spp. as nosocomial pathogens: microbiological, clinical, and epidemiological features. *Clin. Microbiol. Rev.* **9**, 148–165.

Blot, S., Vandewoude, K., and Colardyn, F. 2003. Nosocomial bacteremia involving *Acinetobacter baumannii* in critically ill patients: a matched cohort study. *Intensive Care Med.* **29**, 471–475.

Carratalá, J.V., Serna, N., Villaverde, A., Vázquez, E., and Ferrer-Miralles, N. 2020. Nanostructured antimicrobial peptides: the last push towards clinics. *Biotechnol. Adv.* **44**, 107603.

Cerqueira, G.M. and Peleg, A.Y. 2011. Insights into *Acinetobacter baumannii* pathogenicity. *IUBMB Life* **63**, 1055–1060.

Cheng, M.M.C., Cuda, G., Bunimovich, Y.L., Gaspari, M., Heath, J.R., Hill, H.D., Mirkin, C.A., Nijdam, A.J., Terracciano, R., Thundat, T., *et al.* 2006. Nanotechnologies for biomolecular detection and medical diagnostics. *Curr. Opin. Chem. Biol.* **10**, 11–19.

Choi, J., Baek, J., Kweon, D., Ko, K.S., and Yoon, H. 2020. Rapid determination of carbapenem resistance by low-cost colorimetric methods: propidium Iodide and alamar blue staining. *J. Microbiol.* **58**, 415–421.

Choi, C.H., Lee, J.S., Lee, Y.C., Park, T.I., and Lee, J.C. 2008. *Acinetobacter baumannii* invades epithelial cells and outer membrane protein A mediates interactions with epithelial cells. *BMC Microbiol.* **8**, 216.

Connor, E.E., Mwamuka, J., Gole, A., Murphy, C.J., and Wyatt, M.D. 2005. Gold nanoparticles are taken up by human cells but do not cause acute cytotoxicity. *Small* **1**, 325–327.

Darouiche, R.O. and Hamill, R.J. 1994. Antibiotic penetration of and bactericidal activity within endothelial cells. *Antimicrob. Agents Chemother.* **38**, 1059–1064.

De Vegas, E.Z.S., Nieves, B., Araque, M., Velasco, E., Ruíz, J., and Vila, J. 2006. Outbreak of infection with *Acinetobacter* strain RUH 1139 in an intensive care unit. *Infect. Control Hosp. Epidemiol.* **27**, 397–403.

Dijkshoorn, L., Nemec, A., and Seifert, H. 2007. An increasing threat in hospitals: multidrug-resistant *Acinetobacter baumannii*. *Nat. Rev. Microbiol.* **5**, 939–951.

Esposito, S., Tagliabue, C., Bosis, S., and Principi, N. 2011. Levofloxacin for the treatment of *Mycoplasma pneumoniae*-associated meningoencephalitis in childhood. *Int. J. Antimicrob. Agents* **37**, 472–475.

Fagon, J.Y., Chastre, J., Domart, Y., Trouillet, J.L., and Gibert, C. 1996. Mortality due to ventilator-associated pneumonia or colonization with *Pseudomonas* or *Acinetobacter* species: assessment by quantitative culture of samples obtained by a protected specimen brush. *Clin. Infect. Dis.* **23**, 538–542.

Fair, R.J. and Tor, Y. 2014. Antibiotics and bacterial resistance in the 21st century. *Perspect. Medicin. Chem.* **6**, 25–64.

Gaddy, J.A., Tomaras, A.P., and Actis, L.A. 2009. The *Acinetobacter baumannii* 19606 OmpA protein plays a role in biofilm formation on abiotic surfaces and in the interaction of this pathogen with eukaryotic cells. *Infect. Immun.* **77**, 3150–3160.

Garnacho-Montero, J., Ortiz-Leyba, C., Jiménez-Jiménez, F., Barrero-Almódovar, A., García-Garmendia, J., Bernabeu-Wittell, M., Gallego-Lara, S., and Madrazo-Osuna, J. 2003. Treatment of multidrug-resistant *Acinetobacter baumannii* ventilator-associated

pneumonia (VAP) with intravenous colistin: a comparison with imipenem-susceptible VAP. *Clin. Infect. Dis.* **36**, 1111–1118.
Gentilucci, L., Tolomelli, A., and Squassabia, F. 2006. Peptides and peptidomimetics in medicine, surgery and biotechnology. *Curr. Med. Chem.* **13**, 2449–2466.
Hancock, R.E.W. and Sahl, H.G. 2006. Antimicrobial and host-defense peptides as new anti-infective therapeutic strategies. *Nat. Biotechnol.* **24**, 1551–1557.
Jawad, A., Seifert, H., Snelling, A., Heritage, J., and Hawkey, P.M. 1998. Survival of *Acinetobacter baumannii* on dry surfaces: comparison of outbreak and sporadic isolates. *J. Clin. Microbiol.* **36**, 1938–1941.
Jiang, Q., Lou, Z., Wang, H., and Chen, C. 2019. Antimicrobial effect and proposed action mechanism of cordycepin against *Escherichia coli* and *Bacillus subtilis*. *J. Microbiol.* **57**, 288–297.
Kang, H.K., Kim, C., Seo, C.H., and Park, Y. 2017. The therapeutic applications of antimicrobial peptides (AMPs): a patent review. *J. Microbiol.* **55**, 1–12.
Kang, S.J., Park, S.J., Mishig-Ochir, T., and Lee, B.J. 2014. Antimicrobial peptides: therapeutic potentials. *Expert Rev. Anti Infect. Ther.* **12**, 1477–1486.
Kim, S.M., Escorbar, I., Lee, K., Fuchs, B.B., Mylonakis, E., and Kim, W. 2020. Anti-MRSA agent discovery using *Caenorhabditis elegans*-based high-throughput screening. *J. Microbiol.* **58**, 431–444.
Kim, S.Y., Park, C., Jang, H.J., Kim, B.O., Bae, H.W., Chung, I.Y., Kim, E.S., and Cho, Y.H. 2019. Antibacterial strategies inspired by the oxidative stress and response networks. *J. Microbiol.* **57**, 203–212.
Kim, M., Park, J., Kang, M., Yang, J., and Park, W. 2021. Gain and loss of antibiotic resistant genes in multidrug resistant bacteria: One Health perspective. *J. Microbiol.* **59**, 535–545.
Ko, K.S. 2019. Antibiotic-resistant clones in Gram-negative pathogens: presence of global clones in Korea. *J. Microbiol.* **57**, 195–202.
Kökpinar, Ö., Walter, J.G., Shoham, Y., Stahl, F., and Scheper, T. 2011. Aptamer-based downstream processing of his-tagged proteins utilizing magnetic beads. *Biotechnol. Bioeng.* **108**, 2371–2379.
Kramer, A., Schwebke, I., and Kampf, G. 2006. How long do nosocomial pathogens persist on inanimate surfaces? A systematic review. *BMC Infect. Dis.* **6**, 130.
Lai, M.J., Lin, N.T., Hu, A., Soo, P.C., Chen, L.K., Chen, L.H., and Chang, K.C. 2011. Antibacterial activity of *Acinetobacter baumannii* phage ϕAB2 endolysin (LysAB2) against both Gram-positive and Gram-negative bacteria. *Appl. Microbiol. Biotechnol.* **90**, 529–539.
Lee, K., Kim, D.W., and Cha, C.J. 2021. Overview of bioinformatic methods for analysis of antibiotic resistome from genome and metagenome data. *J. Microbiol.* **59**, 270–280.
Lee, H.T., Kim, S.K., and Yoon, J.W. 2019. Antisense peptide nucleic acids as a potential anti-infective agent. *J. Microbiol.* **57**, 423–430.
Lee, B., Park, J., Ryu, M., Kim, S., Joo, M., Yeom, J.H., Kim, S., Park, Y., Lee, K., and Bae, J. 2017. Antimicrobial peptide-loaded gold nanoparticle-DNA aptamer conjugates as highly effective antibacterial therapeutics against *Vibrio vulnificus*. *Sci. Rep.* **7**, 13572.
Lehar, S.M., Pillow, T., Xu, M., Staben, L., Kajihara, K.K., Vandlen, R., DePalatis, L., Raab, H., Hazenbos, W.L., Morisaki, J.H., *et al.* 2015. Novel antibody-antibiotic conjugate eliminates intracellular *S. aureus*. *Nature* **527**, 323–328.
Lemon, D.J., Kay, M.K., Titus, J.K., Ford, A.A., Chen, W., Hamlin, N.J., and Hwang, Y.Y. 2019. Construction of a genetically modified T7Select phage system to express the antimicrobial peptide 1018. *J. Microbiol.* **57**, 532–538.
Mahgoub, S., Ahmed, J., and Glatt, A.E. 2002. Underlying characteristics of patients harboring highly resistant *Acinetobacter baumannii*. *Am. J. Infect. Control* **30**, 386–390.
Makabenta, J.M.V., Nabawy, A., Li, C.H., Schmidt-Malan, S., Patel, R., and Rotello, V.M. 2021. Nanomaterial-based therapeutics for antibiotic-resistant bacterial infections. *Nat. Rev. Microbiol.* **19**, 23–36.
Marr, A.K., Gooderham, W.J., and Hancock, R.E. 2006. Antibacterial peptides for therapeutic use: obstacles and realistic outlook. *Curr. Opin. Pharmacol.* **6**, 468–472.
McConnell, M.J., Domínguez-Herrera, J., Smani, Y., López-Rojas, R., Docobo-Pérez, F., and Pachón, J. 2011. Vaccination with outer membrane complexes elicits rapid protective immunity to multidrug-resistant *Acinetobacter baumannii*. *Infect. Immun.* **79**, 518–526.
Mishra, B., Reiling, S., Zarena, D., and Wang, G. 2017. Host defense antimicrobial peptides as antibiotics: design and application strategies. *Curr. Opin. Chem. Biol.* **38**, 87–96.
Mukhopadhyay, S., Prasad, A.S.B., Mehta, C.H., and Nayak, U.Y. 2020. Antimicrobial peptide polymers: No escape to ESKAPE pathogens–a review. *World J. Microbiol. Biotechnol.* **36**, 131.
Nordström, R. and Malmsten, M. 2017. Delivery systems for antimicrobial peptides. *Adv. Colloid Interface Sci.* **242**, 17–34.
Paleos, C.M., Tsiourvas, D., Sideratou, Z., and Tziveleka, L. 2004. Acid-and salt-triggered multifunctional poly (propylene imine) dendrimer as a prospective drug delivery system. *Biomacromolecules* **5**, 524–529.
Park, Y.K., Lee, G.H., Baek, J.Y., Chung, D.R., Peck, K.R., Song, J.H., and Ko, K.S. 2010. A single clone of *Acinetobacter baumannii*, ST22, is responsible for high antimicrobial resistance rates of *Acinetobacter* spp. isolates that cause bacteremia and urinary tract infections in Korea. *Microb. Drug Resist.* **16**, 143–149.
Parra-Millán, R., Guerrero-Gómez, D., Ayerbe-Algaba, R., Pachón-Ibáñez, M.E., Miranda-Vizuete, A., Pachón, J., and Smani, Y. 2018. Intracellular trafficking and persistence of *Acinetobacter baumannii* requires transcription factor EB. *mSphere* **3**, e00106-18.
Peleg, A.Y., Seifert, H., and Paterson, D.L. 2008. *Acinetobacter baumannii*: emergence of a successful pathogen. *Clin. Microbiol. Rev.* **21**, 538–582.
Peng, S.Y., You, R.I., Lai, M.J., Lin, N.T., Chen, L.K., and Chang, K.C. 2017. Highly potent antimicrobial modified peptides derived from the *Acinetobacter baumannii* phage endolysin LysAB2. *Sci. Rep.* **7**, 11477.
Perez, F., Hujer, A.M., Hujer, K.M., Decker, B.K., Rather, P.N., and Bonomo, R.A. 2007. Global challenge of multidrug-resistant *Acinetobacter baumannii*. *Antimicrob. Agents Chemother.* **51**, 3471–3484.
Projan, S.J. 2003. Why is big Pharma getting out of antibacterial drug discovery? *Curr. Opin. Microbiol.* **6**, 427–430.
Qiu, H., KuoLee, R., Harris, G., Van Rooijen, N., Patel, G.B., and Chen, W. 2012. Role of macrophages in early host resistance to respiratory *Acinetobacter baumannii* infection. *PLoS ONE* **7**, e40019.
Rice, L.B. 2008. Federal funding for the study of antimicrobial resistance in nosocomial pathogens: no ESKAPE. The University of Chicago Press. Chicago, Illinois, USA.
Rolain, J.M., Diene, S.M., Kempf, M., Gimenez, G., Robert, C., and Raoult, D. 2013. Real-time sequencing to decipher the molecular mechanism of resistance of a clinical pan-drug-resistant *Acinetobacter baumannii* isolate from Marseille, France. *Antimicrob. Agents Chemother.* **57**, 592–596.
Roscia, G., Falciani, C., Bracci, L., and Pini, A. 2013. The development of antimicrobial peptides as new antibacterial drugs. *Curr. Protein Pept. Sci.* **14**, 641–649.
Rosi, N.L. and Mirkin, C.A. 2005. Nanostructures in biodiagnostics. *Chem. Rev.* **105**, 1547–1562.
Ryu, M., Park, J., Yeom, J.H., Joo, M., and Lee, K. 2021. Rediscovery of antimicrobial peptides as therapeutic agents. *J. Microbiol.* **59**, 113–123.
Schmid, G. 1992. Large clusters and colloids. Metals in the embryonic state. *Chem. Rev.* **92**, 1709–1727.
Shin, B. and Park, W. 2017. Antibiotic resistance of pathogenic *Acin-*

etobacter species and emerging combination therapy. *J. Microbiol.* **55**, 837–849.

Theaker, C., Azadian, B., and Soni, N. 2003. The impact of *Acinetobacter baumannii* in the intensive care unit. *Anaesthesia* **58**, 271–274.

Valero, C., Palomo, J.D.G., Matorras, P., Fernández-Mazarrasa, C., Fernández, C.G., and Fariñas, M.C. 2001. *Acinetobacter bacteraemia* in a teaching hospital, 1989–1998. *Eur. J. Intern. Med.* **12**, 425–429.

Wang, S.H., Sheng, W.H., Chang, Y.Y., Wang, L.H., Lin, H.C., Chen, M.L., Pan, H.J., Ko, W.J., Chang, S.C., and Lin, F.Y. 2003. Healthcare-associated outbreak due to pan-drug resistant *Acinetobacter baumannii* in a surgical intensive care unit. *J. Hosp. Infect.* **53**, 97–102.

Wróblewska, M. 2006. Novel therapies of multidrug-resistant *Pseudomonas aeruginosa* and *Acinetobacter* spp. infections: the state of the art. *Arch. Immunol. Ther. Exp.* **54**, 113–120.

Xiong, M.H., Bao, Y., Yang, X.Z., Zhu, Y.H., and Wang, J. 2014. Delivery of antibiotics with polymeric particles. *Adv. Drug Deliv. Rev.* **78**, 63–76.

Yeom, J.H., Lee, B., Kim, D., Lee, J., Kim, S., Bae, J., Park, Y., and Lee, K. 2016. Gold nanoparticle-DNA aptamer conjugate-assisted delivery of antimicrobial peptide effectively eliminates intracellular *Salmonella enterica* serovar Typhimurium. *Biomaterials* **104**, 43–51.

Yeung, A.T.Y., Gellatly, S.L., and Hancock, R.E. 2011. Multifunctional cationic host defence peptides and their clinical applications. *Cell. Mol. Life Sci.* **68**, 2161.